THE JOURNAL OF BIOLOGICAL CHEMISTRY VOL. 282, NO. 31, pp. 22921–22929, August 3, 2007

ATP-induced Structural Transitions in PAN, the Proteasome-regulatory ATPase Complex in Archaea*

Received for publication, April 3, 2007, and in revised form, June 1, 2007 Published, JBC Papers in Press, June 6, 2007, DOI 10.1074/jbc.M702846200

Andrew A. Horwitz[‡1], **Ami Navon**[§1], **Michael Groll**[¶], **David M. Smith**[‖], **Christian Reis**[‖], **and Alfred L. Goldberg**[‖2]

From the [‡]*Program in Biology and Biomedical Sciences and the* [‖]*Department of Cell Biology, Harvard Medical School, Boston, Massachusetts 02115, the* [§]*Department of Biological Regulation, Weizmann Institute, Rehovot 76100, Israel, and the* [¶]*Institute of Biochemistry, Charité-Universitatsmedizin Berlin CCM, Monbijoustrasse 2, 10117 Berlin, Germany*

ATP binding to the PAN-ATPase complex in Archaea or the homologous 19 S protease-regulatory complex in eukaryotes induces association with the 20 S proteasome and opening of its substrate entry channel, whereas ATP hydrolysis allows unfolding of globular substrates. To clarify the conformational changes associated with ATP binding and hydrolysis, we used protease sensitivity to monitor the conformations of the PAN ATPase from *Methanococcus jannischii*. Exhaustive trypsin treatment of PAN generated five distinct fragments, two of which differed when a nucleotide (either ATP, ATPγS, or ADP) was bound. Surprisingly, the nucleotide concentrations altering protease sensitivity were much lower (K_a 20–40 μM) than are required for ATP-dependent protein breakdown by the PAN-20S proteasome complex ($K_m \sim$ 300–500 μM). Unlike trypsin, proteinase K yielded several fragments that differed in the ATPγS and ADP-bound forms, and thus revealed conformational transitions associated with ATP hydrolysis. Mapping the fragments generated by each revealed that nucleotide binding and hydrolysis induce local conformational changes, affecting the Walker A and B nucleotide-binding motif, as well as global changes extending to its carboxyl terminus. The location and overlap of the fragments also suggest that the conformation of the six subunits is not identical, probably because they do not all bind ATP simultaneously. Partial nucleotide occupancy was supported by direct assays, which demonstrated that, at saturating conditions, only four nucleotides are bound to hexameric PAN. Using the protease protection maps, we modeled the conformational changes associated with ATP binding and hydrolysis in PAN based on the x-ray structures of the homologous AAA ATPase, HslU.

In both prokaryotic and eukaryotic cells, most proteins are degraded in an ATP-dependent manner (1, 2). In eukaryotes, ATP-dependent degradation is catalyzed by the 26 S proteasome, which hydrolyzes ubiquitin-conjugated and some non-ubiquitinated proteins (3, 4). In this process, polyubiquitinated proteins bind the 19 S regulatory particle, which is believed to promote their unfolding and translocation into the 20 S core particle (5, 6), where hydrolysis to small peptides occurs. The 19 S complex contains six homologous ATPases in its base, which lies adjacent to the 20 S particle. These ATPases have been implicated in substrate recognition, unfolding, translocation, and gate opening in the outer ring of the 20 S particle (5–10).

Although prokaryotes lack ubiquitin and 26 S proteasomes, archaebacteria do have 20 S proteasomes, whose architecture and proteolytic mechanism closely resemble those of the eukaryotic 20 S (11). Because of its greater simplicity, the archaeal 20 S proteasome has proven very useful for structural and mechanistic studies (12–14). The Archaea proteasome functions in protein breakdown in association with an ATPase complex, termed PAN[3] (proteasome-activating nucleotidase). When mixed with the archaeal 20 S proteasome and ATP, PAN stimulates the degradation of natively unfolded proteins and peptides longer than 7 residues, whereas shorter peptides diffuse into the 20 S proteasome unassisted (11). PAN is a hexameric ring with a central pore, and thus its general structure resembles that of the six ATPases of the 19 S complex (6). Like them, PAN exhibits several typical chaperone properties, including the ability to bind unfolded polypeptides selectively and to prevent their aggregation (15–17). In addition, in the presence of ATP, PAN efficiently unfolds certain globular substrates and translocates them into the 20 S proteasome (17).

PAN shows 40% homology to the six ATPases in the base of the 19 S particle and thus appears to have regulated proteasome function prior to the linkage of ubiquitination and proteolysis (11). Both proteasome-regulatory complexes are members of the AAA superfamily of multimeric ATPases, which also includes the ATP-dependent proteases Lon and FtsH and the regulatory components of the bacterial ATP-dependent proteases ClpAP, ClpXP, and HslUV (18, 19). The unifying feature of the AAA superfamily is an ATPase domain of about 220 amino acids, whose structural fold has been solved by x-ray crystallography (20–22). The AAA proteins show a strong sequence conservation in this domain (about 30% identity), which contains the Walker A and B (ATP binding and hydrolysis) motifs. In addition to ATP-dependent proteolysis, AAA proteins play key roles in diverse processes, from membrane trafficking to microtubule regulation (23, 24).

Despite the importance of the AAA superfamily, their mode of action is not well understood. In particular, the link between

* This work was also supported by a predoctoral fellowship from the Department of Defense Breast Cancer Research Program (to A. A. H.) and research grants (to A. C. G.) from the National Institutes of Health, NINDS. The costs of publication of this article were defrayed in part by the payment of page charges. This article must therefore be hereby marked "*advertisement*" in accordance with 18 U.S.C. Section 1734 solely to indicate this fact.

[1] Both authors contributed equally to the results of this report.

[2] To whom correspondence should be addressed. E-mail: alfred_goldberg@hms.harvard.edu.

[3] The abbreviations used are: PAN, proteasome-activating nucleotidase; ATPγS, adenosine 5′-*O*-(thiotriphosphate); YFP, yellow fluorescent protein; AMP-PNP, adenosine 5′-(β,γ-imino)triphosphate.

the ATPase catalytic cycle and the conformational changes responsible for their biological activity remain unclear. Here, we focus on PAN, whose simplicity and uniformity offer clear advantages for understanding the role of ATP in facilitating proteolysis (9, 17). The degradation of a globular protein by the PAN-20S complex occurs in multiple steps (6): 1) ATPase association with the 20 S particle; 2) opening of the substrate entry channel in the 20 S proteasome; 3) binding of the substrate to the ATPase; 4) global unfolding of the substrate on the ATPase surface; and 5) processive translocation of the unfolded substrate into the 20 S particle. These functions must be mediated by specific conformational transitions in the ATPase complex upon ATP binding, hydrolysis to ADP, or exchange of ADP for ATP, and a full understanding of ATP-dependent proteolysis will require the resolution of the structural changes associated with each step. Whereas subunit interactions of 19 S subunits have been mapped by cross-linking, mutational analysis, or yeast two-hybrid approaches, nothing is known of how ATP binding and hydrolysis affects the structure of the eukaryotic 19 S particle or the homologous PAN ATPase complex (25–29).

To investigate the influence of nucleotide binding and hydrolysis on the conformation of PAN, we monitored its susceptibility to different proteases in the absence or presence of ATP, ATPγS (a non-hydrolyzable ATP analog), or ADP, and mapped the protease-resistant domains by Edman degradation. Further studies of the sensitivity of PAN to proteinase K uncovered distinct conformations corresponding to the ATPγS-bound and ADP-bound forms, indicating conformational transitions coupled to ATP hydrolysis. Using the solved structures of a homologous AAA family member, we were able to model the main parts of the PAN molecule and the kinds of conformational changes induced by nucleotides.

MATERIALS AND METHODS

Protein Purification—Untagged PAN and mutants were purified to homogeneity from *Escherichia coli* transformed with pRSET plasmid, as previously described (9). Gel filtration analysis indicates that these preparations do not contain monomeric PAN.[4] Additionally, these preparations bind the 20 S proteasome stoichiometrically (6).

Protease Protection—2 μg of PAN (275 nM) was diluted in the digest buffer (15 mM Tris, pH 8.0, 30 mM KCl, 5 mM $MgCl_2$, with or without 2 mM ATP, ADP, or ATPγS) and preincubated 10 min at 20 °C. Protease was added at 30 μg/ml (1.25 μM) Calbiochem trypsin) or 600 ng/ml (207 nM) (Novagen proteinase K) and samples were incubated at 20 °C for 30 min. Digested samples were immediately run on SDS-PAGE and stained with Coomassie Blue.

YFP Degradation Assay—YFP-ssrA was used as a substrate for degradation by PAN and 20 S proteasome, as previously described (9).

Peptide Mapping—Following digestion and SDS-PAGE, protein samples were transferred to a polyvinylidene difluoride membrane, stained with Ponceau, and excised for Edman degradation at the Dana-Farber core sequencing facility.

[4] D. M. Smith and A. L. Goldberg, unpublished observation.

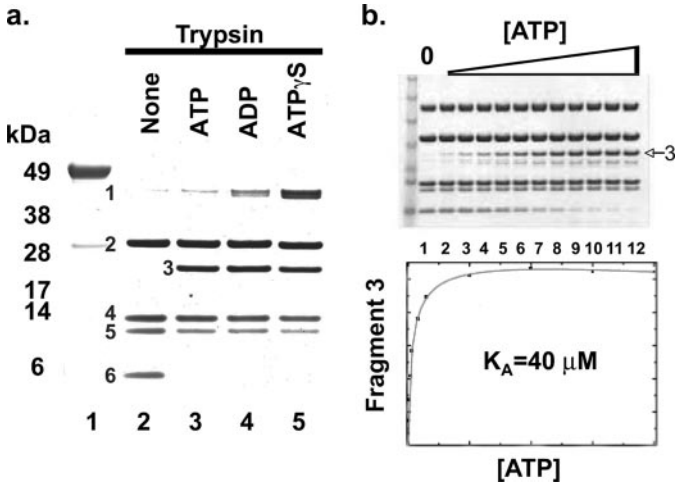

FIGURE 1. **The presence of ATP, ADP, or ATPγS alters the fragments of PAN generated by trypsin digestion.** *a*, PAN was digested with 30 μg/ml trypsin for 30 min, with the addition of 2 mM ATP, ADP, or ATPγS. *Lane 1*, undigested PAN; *lane 2*, trypsin digest, no nucleotide; *lane 3*, trypsin digest, ATP; *lane 4*, trypsin digest, ADP; *lane 5*, trypsin digest, ATPγS. Digestion without any nucleotide yielded bands of 43.5, 30, 14, 12, and 10.5 kDa in size. Addition of nucleotide resulted in the disappearance of the 10.5-kDa band and appearance of a new 25.5-kDa band. *b*, the affinity of PAN for ATP, ADP, and ATPγS were determined by protease protection. The affinity for nucleotide binding to PAN was measured by conducting protease protection assays with increasing concentrations of these nucleotides: *lane 1*, 0 μM; *lane 2*, 2 μM; *lane 3*, 4 μM; *lane 4*, 8 μM; *lane 5*, 16 μM; *lane 6*, 32 μM; *lane 7*, 75 μM; *lane 8*, 150 μM; *lane 9*; 500 μM; *lane 10*, 500 μM; *lane 11*, 1000 μM; *lane 12*, 2000 μM. The protease fragments were separated by SDS-PAGE and stained with Coomassie Blue. The appearance of the 25.5-kDa nucleotide-specific band (denoted by an *arrow*) was quantified by densitometry, plotted against nucleotide concentration, and fitted to the Michaelis-Menten model. Data for only the experiment with ATP is shown, where a K_a of 40 μM was determined.

Kinetics—PAN was digested as described, with 0–2 mM ATP, ADP, or ATPγS. Gels were scanned, and band density was determined with Scanalytics One-Dscan 2.03 software. These data were graphed and Michaelis-Menten kinetics were determined.

Nucleotide Binding Assay—^{35}S-Labeled ATPγS bound to PAN was separated from free nucleotide using a rapid spin column technique as described (30). Various concentrations of PAN were incubated at 37 °C with a minimal 10-fold higher concentration of ATPγ^{35}S (10 mCi/ml, 1200 Ci/mmol, from Amersham Biosciences). Recovery of PAN from the column was 95% as determined by Bradford protein assay and activity assay. The concentration of bound nucleotide was determined by comparing the total counts of the control 1 mM ATPγ^{35}S solution with the number of counts bound to PAN.

RESULTS

To identify the conformational transitions in PAN that result from nucleotide binding and hydrolysis, five different proteolytic enzymes were initially tested: trypsin, chymotrypsin, elastase, V8, and proteinase K (data not shown). Of these, trypsin digestion of PAN for 20 min at 20 °C proved to be the most informative and reproducible. This digest yielded 5 distinct fragments of the following sizes: 43.5 (Tryp 1), 30.3 (Tryp 2), 14 (Tryp 4), 12 (Tryp 5), and 10.6 kDa (Tryp 6) (Fig. 1*A*, *lane 2*), which resisted further digestion when increasing amounts of trypsin (from 30 to 60 μg/ml) were added (data not shown). Tryp 1 was always present, although its amount varied some-

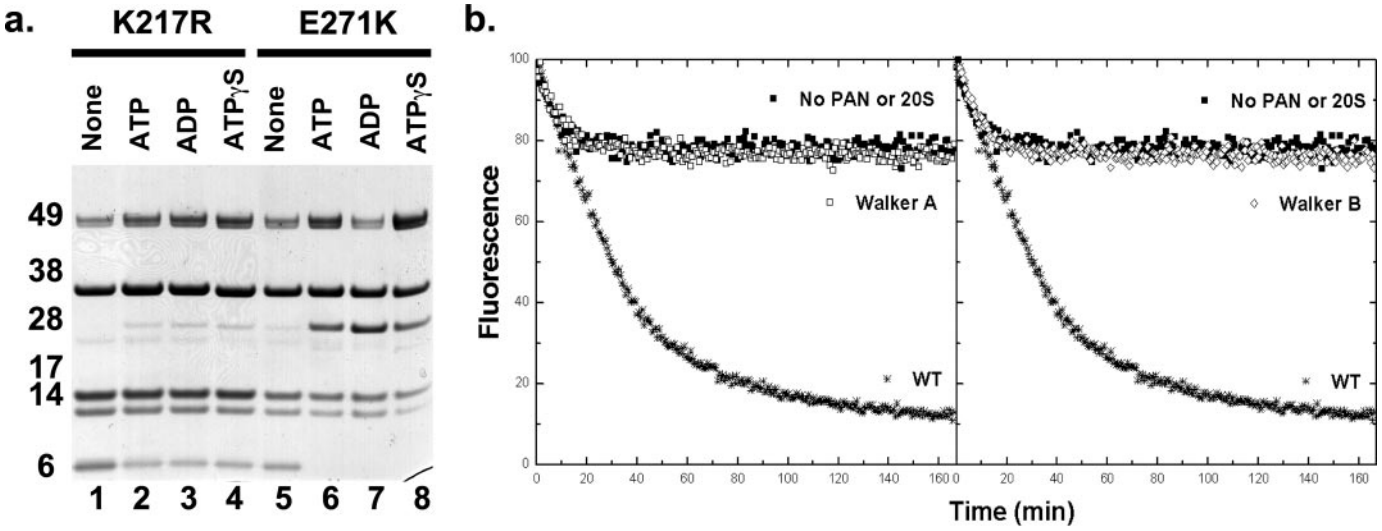

FIGURE 2. **Nucleotide binding, but not hydrolysis, is required to alter the susceptibility of PAN to trypsin.** *a*, mutations in the conserved P loop of PAN, which disrupt ATP binding, but not hydrolysis, blocked the nucleotide-induced conformational change. PAN mutants with a K217R substitution (Walker A motif), or an E271Q substitution (Walker B motif) were purified and analyzed by trypsin digestion as described in the legend Fig. 1. *b*, PAN K217R and E271K variants are defective in unfolding YFP-ssrA. PAN (or mutants) and 20 S proteasomes were incubated with YFP-ssrA in buffer containing 2 mM ATP at 45 °C for 160 min. YFP fluorescence was monitored with a plate reader. A loss of fluorescence (~20%) is observed in the absence of PAN and 20 S, which can be attributed to thermal quenching of the YFP fluorophore upon transition to 45 °C.

what between assays. We attempted to study the generation of these fragments further by conducting time courses of PAN digestion with trypsin. Unfortunately, we were unable to control the reaction sufficiently to study digestion intermediates. Consequently, we have focused in this study on the protease-resistant domains produced by prolonged incubation with trypsin.

To test the effects of nucleotides on trypsin sensitivity, we determined whether the digestion products differed after pre-incubation of PAN with ATP, ADP, or ATPγS. Each of these nucleotides altered the pattern of fragments produced, and, surprisingly, they caused an almost identical set of changes. The pattern of fragments in the presence or absence of a nucleotide differed in two ways. With the addition of each nucleotide, a new product of 25.5 kDa (Tryp 3) appeared, and the smallest peptide (Tryp 6) disappeared (Fig. 1*A*, *lanes 3–5*). These nucleotide-induced alterations reflect changes in the accessibility of trypsin sites and thus indicate conformational changes in PAN.

To define the affinity of the binding site responsible for the changes in susceptibility to trypsin, we incubated PAN with increasing concentrations of ATP, ADP, or ATPγS, followed by exhaustive digestion with trypsin and analysis by SDS-PAGE. The Coomassie-stained gels were scanned, and the Tryp 3 band, which was produced specifically in the presence of nucleotides, was quantified by densitometery (representative data with ATP is shown in Fig. 1*B*). When the amounts of this band were plotted against nucleotide concentration, in each case a clear saturation curve was obtained that could be fitted accurately with a model assuming saturable binding of the nucleotide to inhibit cleavage by trypsin. The concentrations of these nucleotides that gave half-maximal production of Tryp 3 were very similar: K_a for ATP = 40 μM, ADP = 27 μM, ATPγS = 22 μM. These changes in sensitivity were due to nucleotide binding to PAN, and not to some effect on trypsin activity, because in control experiments, increasing concentrations of ATP caused no change in the rate of casein hydrolysis by trypsin or the nature of the products generated (data not shown). Surprisingly, the K_a of PAN for these nucleotides (~20–40 μM) was much lower than the K_m previously determined for the ATP-dependent breakdown of casein by the PAN-20S complex (~500 μM) (31) or at 300 μM.[5]

To confirm that the high affinity binding of nucleotides to PAN is dependent on the Walker A and Walker B motifs (amino acids 211–273), we engineered two variants of PAN (32–34). First, we substituted an arginine for the conserved lysine (K217R) in the Walker A domain, which in other ATPases is necessary for nucleotide binding. The pattern of peptides generated upon incubation of this Walker A mutant with trypsin was minimally affected by the presence of any of the nucleotides (Fig. 2*A*, *lanes 1–4*). Although Tryp 3 was generated at low efficiency in the presence of a nucleotide, this may indicate that a small degree of nucleotide binding occurs in the K217R mutant. We also inserted a glutamine for the glutamic acid (E271Q) in the Walker B motif, which is required for ATP hydrolysis in other ATPases. The Walker B mutant in PAN exhibited the same changes in trypsin sensitivity upon addition of ATP, ADP, or ATPγS as the unmodified PAN (Fig. 2*A*, *lanes 5–8*). Therefore, the conformational changes detected by the trypsin protection assay require nucleotide binding at the Walker A motif, but not ATP hydrolysis, as was also suggested by the identical products obtained with ADP and ATPγS.

To confirm that these mutations were affecting the capacity of PAN to support ATP-dependent protein degradation by the 20 S particle, we assayed the degradation of an YFP-ssrA fusion protein (Fig. 2*B*). Unmodified PAN catalyzed the ATP-dependent degradation of YFP-ssrA by the 20 S, as shown by the reduction in green fluorescence protein fluorescence. However, nei-

[5] N. Ng and A. L. Goldberg, unpublished observations.

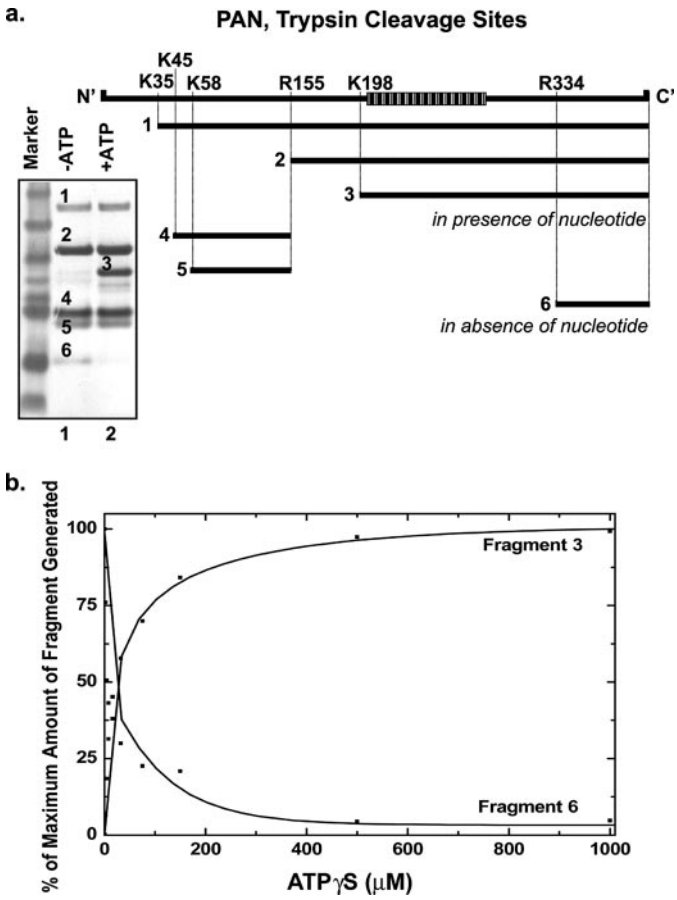

FIGURE 3. **Mapping trypsin fragments reveals reciprocal relationships between certain nucleotide-sensitive fragments.** *a*, trypsin digestion of PAN with (*lane 1*) or without (*lane 2*) ATP present yielded fragments that were identified by Edman degradation and are shown on a map of PAN. The P-loop containing the Walker A motif is depicted as a *shaded bar*. *b*, nucleotide-sensitive fragments Tryp 3 and Tryp 6 are derived from a common precursor. The relative quantity of Tryp 3 and Tryp 6 (Fig. 1*b*) was determined by densitometry and plotted as percentage of total against the ADP concentration.

ther the Walker A nor Walker B mutants showed any activity. Thus, both conformational changes detected by trypsin and ATP-dependent proteolysis require the same ATP-binding site, even though these events occur at different concentrations of the nucleotide.

To define the protease-resistant domains and localize the conformational changes in PAN upon nucleotide binding, we used Edman degradation to map the stable products generated by trypsin. A unique amino-terminal sequence was found for each fragment (Fig. 3*A*). Only a small fraction of the arginine or lysine residues in PAN were cleaved by trypsin, and all the fragments that were resistant to trypsin contained an additional potential cleavage sites that presumably were protected by the structure of the domain. The Tryp 1 (395 amino acids) and Tryp 2 (275 amino acids) fragments, observed in the presence or absence of a nucleotide, lack the NH_2-terminal 35 and 155 amino acids, respectively. The first 35 residues, which are largely charged, were not recovered in any fragment, and likely correspond to a trypsin-sensitive region with a loose structure. Tryp 3, a COOH-terminal fragment of 232 amino acids was observed only in the presence of nucleotides. The nearly identical Tryp 4 (127 amino acids) and Tryp 5 (109 amino acids) were observed regardless of nucleotide, and are located near the NH_2 terminus of Tryp 1. The second nucleotide-sensitive fragment, COOH-terminal Tryp 6 (96 amino acids), disappeared in the presence of nucleotide.

The location of the nucleotide-sensitive fragments Tryp 3 and Tryp 6 suggests that nucleotide-induced conformational changes occur both locally (around the Walker A and B domains) and globally (throughout the protein). The NH_2 terminus of Tryp 3 is located in the vicinity of the Walker A and B motif and thus its generation could be directly affected by local structural changes accompanying nucleotide binding. Tryp 6, however, is over 60 amino acids away from the COOH-terminal end of the Walker A and B motif and 136 amino acids from the NH_2 terminus of Tryp 3. Its disappearance after binding of a nucleotide requires an alteration in the carboxyl-terminal region of the PAN monomers. Although it is possible that Arg^{334} (Tryp 6 cleavage site) is actually adjacent to the Walker motifs in the three-dimensional structure, this cleavage indicates that nucleotide binding has global effects on the structure of PAN.

Overlapping Trypsin Fragments Support the Existence of Multiple Monomer Conformations—Although Tryp 3 and Tryp 6 overlap in sequence with the nucleotide-insensitive Tryp 2, the generation of Tryp 3 in the presence of a nucleotide cannot occur via further processing of Tryp 2. As shown in Fig. 1*B*, the addition of nucleotides generated increasing amounts of Tryp 3 without affecting the amount of Tryp 2. By contrast, Tryp 3 and Tryp 6 seem to be generated by alternative processing of a common precursor, because the accumulation of Tryp 3 correlated directly with the disappearance of Tryp 6. It follows that Tryp 3 and Tryp 6 must be generated from different monomers than those that generate Tryp 2. To further analyze the relationship between the nucleotide-sensitive Tryp 3 and Tryp 6, we determined the quantity of each fragment in Fig. 1*B* by densitometry, and plotted the percent of maximum fragment generated against the concentration of ATP in the reaction (Fig. 3*B*). The intersection of these plots occurs near the 50% maximum of each of the fragments, supporting the notion that fragments 3 and 6 are generated from the same full-length monomer (*i.e.* at the expense of each other). Furthermore, the concentration at which this intersection occurs is similar to the K_a of PAN for nucleotide (~40 μM ATPγS).

All Six PAN Subunits Do Not Bind ATPγS Simultaneously—These results strongly suggest that although PAN is a homohexamer, individual subunits can adopt alternate conformations. The simplest mechanism by which heterogeneity in the homohexameric ring might arise would be if some subunits bound nucleotides, whereas others did not. To directly test this hypothesis, we measured nucleotide binding to PAN using radiolabeled ATPγS and Sephadex G-50 spin columns to separate PAN from the unbound nucleotide. With increasing amounts of PAN, increasing amounts of ATPγ^{35}S were recovered with PAN in the flow-through. As shown in Fig. 4, the slope of this line indicated binding of exactly four nucleotides per PAN hexamer. These results were obtained at a high concentration of ATPγS (1 mM) that gave maximal binding (data not shown). Thus, these experiments indicate that each PAN hexamer binds a maximum of four ATPγS molecules under

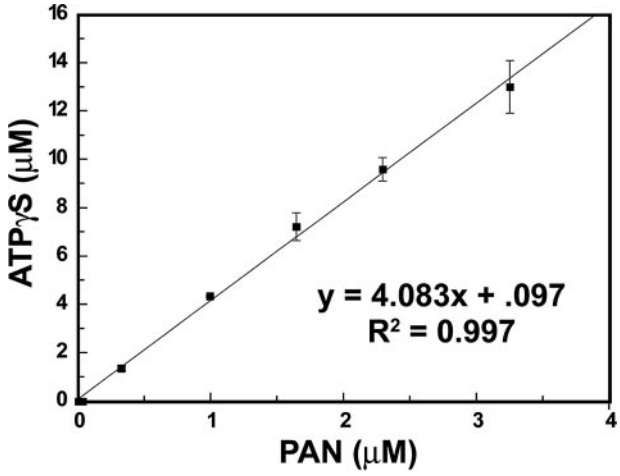

FIGURE 4. **ATPγS binds to, at most, four subunits of PAN as show by the proportionality between PAN concentration and ATPγ^{35}S binding.** Varying concentrations of PAN were incubated at 37 °C with 1 mM ATPγ^{35}S, which gave maximal nucleotide binding (data not shown). Bound nucleotide was separated from free by rapid centrifugation through a Sephadex G-50 column. The *abscissa* represents the concentration of PAN in the flow-through. The *ordinate* shows the concentration of ATPγ^{35}S bound to PAN (recovered in the flow-through). 95% of PAN was recovered in these experiments.

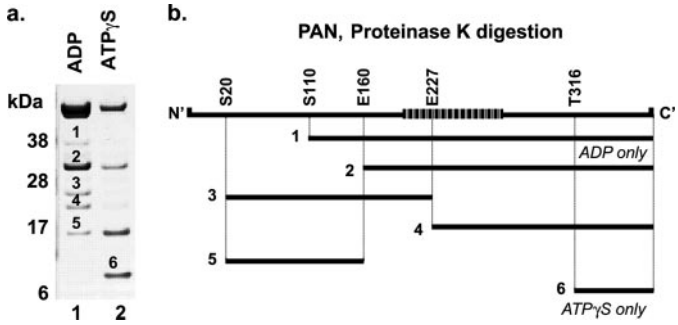

FIGURE 5. **ATP hydrolysis induces conformational changes in PAN detectable by proteinase K digestion.** *a*, proteinase K (0.6 μg/ml) was used to digest 2 μg of PAN in the presence of 2 mM ADP (*lane 1*) or 2 mM ATPγS. Fragments were separated by SDS-PAGE, and stained with Coomassie Blue. *b*, peptide map of proteinase K fragments. The numbered bands (*left panel*) were excised and identified by Edman degradation (*right panel*). The P-loop, containing the Walker A and B motif, is depicted as a *shaded bar*. Prok 1, a COOH-terminal fragment of 320 amino acids, was only observed in the presence of ADP. Prok 2, a COOH-terminal fragment of 270 amino acids, was most abundant with ADP, but was observed to a lesser extent with ATPγS. Prok 3, which corresponds to residues 20–227 and Prok 4, which begins exactly at the COOH terminus of Prok 3 and extends 203 amino acids to the COOH terminus of PAN, were present only with ADP. Prok 5, which shares an NH_2 terminus at residue 20 with Prok 3, but is only 140 amino acids, was most abundant with ATPγS, and was produced to a smaller extent with ADP. Prok 6, a COOH-terminal fragment of 114 amino acids, was observed only in the presence of ATPγS.

saturating conditions (Fig. 4) and support the existence of multiple monomer conformations as suggested by the trypsin fragments (Fig. 4).

Protease Treatment Distinguishes ATPγS- and ADP-bound Forms of PAN—Because the ATPγS- and ADP-bound state of PAN are known to have different functional consequences (6, 7), but did not differ in susceptibility to trypsin, the changes associated with ATP hydrolysis must not expose or conceal a trypsin-sensitive site. We therefore tested other proteases to see if there were any differences in the products generated upon binding of ATPγS and ADP. As shown in Fig. 5*A*, the fragments generated by proteinase K in the presence of ADP (or without a nucleotide, data not shown) differed from those produced with ATPγS. As determined by Edman degradation, the first 20 NH_2-terminal amino acids of PAN were lost after proteinase K treatment, which is further evidence that this NH_2-terminal region is relatively unstructured (Fig. 5*B*). Unfortunately, the fragments generated with proteinase K (in contrast to those with trypsin) were not completely resistant to the protease, and as a result varied in quantity between experiments, and therefore could not be quantitated reliably. A complete description of the fragments is included in the figure legend.

The cleavage patterns clearly indicate that two types of conformational changes were induced by ATPγS. One involved a decrease in the quantity of Prok 3 (which was not found with ATPγS), whereas there was an increase in Prok 5 (which was predominant with ATPγS). The other resulted in the loss of Prok 4 (which was not found with ATPγS) and the appearance of Prok 6 (which was unique to ATPγS). As found with trypsin, the changes monitored with proteinase K digestion involved the complete protein, including the ATP-binding domain. The conformational change leading to the generation of Prok 5 occurs in the Walker A and B regions and therefore can be attributed to local structural changes associated with the loss of the γ-phosphate. By contrast, the generation of Prok 6 suggests a global conformational change, which extends to the very carboxyl terminus of the molecule. These two results indicate a cycle of conformational changes associated with ATP binding and hydrolysis to ADP.

DISCUSSION

In this study, digestions with trypsin and proteinase K have provided complementary information about the structure of PAN and the effects of nucleotide binding and ATP hydrolysis. The trypsin digest is particularly interesting because it indicates that there are multiple monomer conformations in the homohexameric ring. The overlap between fragments Tryp 3 and 6 (Fig. 3*B*) could result from three distinct conformations of the monomer. We propose that the first conformation, "A," yields Tryp 2 upon digestion and is observed in the presence or absence of a nucleotide. In the absence of a nucleotide, a second conformation, "B", yields Tryp 6. Upon addition of nucleotide, the B conformation converts to a third form, "C," which yields Tryp 3. The existence of multiple conformations in a complex is due most likely to nucleotide binding to only some of six subunits of PAN. Partial occupancy of the hexamer by nucleotides was directly confirmed by a nucleotide binding measurement, which indicated that only four ATPγS molecules bound per PAN hexamer at saturating conditions (Fig. 4). The functional consequences of having multiple conformations at any time within the PAN hexamer are an important question for future study especially because the transitions of different subunits between these conformations is likely to underlie the ability of PAN to promote substrate unfolding and translocation.

Thus, the most likely interpretation of these findings is that a single hexamer contains monomers that do not bind nucleotide and maintain the A conformation as well as monomers that are sensitive to nucleotide and can adopt either the B or C conformation. An alternative explanation of the trypsin fragments could be that these preparations contain distinct populations of

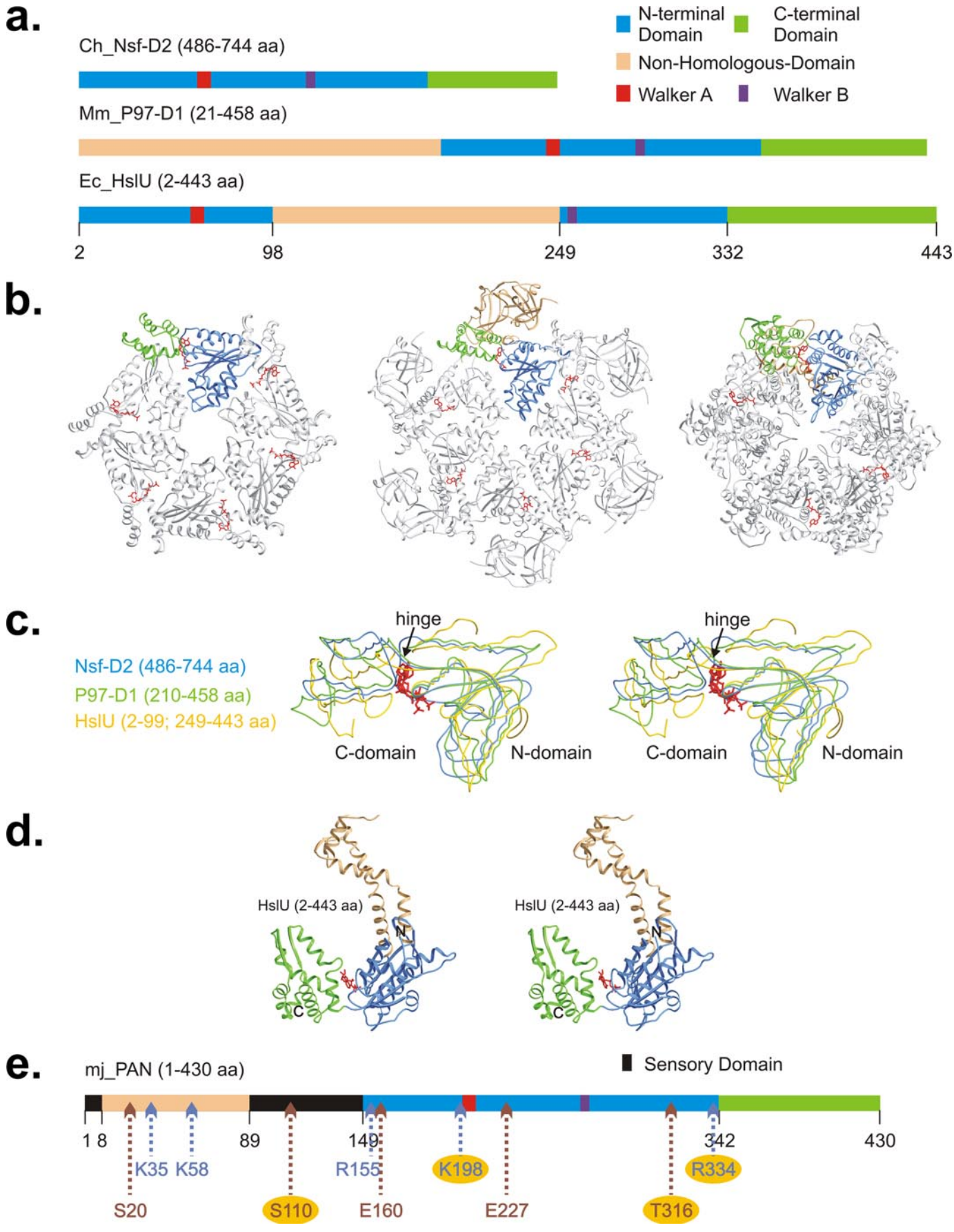

PAN, each comprised wholly of bound and unbound monomers. It is also theoretically possible that stochastic asymmetry in PAN initiates different pathways of trypsin digestion in otherwise identical subunits. However, neither of these possibilities would fit with the nucleotide binding data (Fig. 4) or with extensive unpublished data indicating distinct functional consequences when increasing amounts of ATPγS bind to PAN.[6] Furthermore, there is strong precedent for a partial occupancy arrangement in related AAA ATPases. A study of the AAA ClpX homohexamer demonstrated that subunits are partitioned into three classes with different nucleotide binding and release properties (35). In addition, early studies on ATP binding in the lon (La) protease indicated four nucleotides bound per multimer, which at the time was believed to be tetrameric (30). Because lon is in fact a hexameric AAA family member, these observations are similar to the present findings. In addition, partial nucleotide occupancy has been described in HslU, where the crystal structure reveals AMP-PNP bound to only 4 subunits of the hexamer (21). Thus, it appears most likely that some of the monomers in a PAN hexamer bind nucleotide and undergo conformational transitions whereas others do not.

Comparison of the peptides generated by trypsin and proteinase K reveals several similarities that are informative about the domain structure of PAN. First, both proteases yielded a limited set of fragments that spanned almost the entirety of PAN, but indicated that the majority of potential cleavage sites were inaccessible. However, the first 20–35 residues of PAN, which precede a predicted coiled-coil domain (11), were fully digested regardless of protease or nucleotide tested, confirming that this region lacks significant tertiary structure under any nucleotide condition. Although proteinase K has a much wider substrate range than trypsin, both yielded similar nucleotide-resistant fragments, suggesting that the regions cleaved correspond to loops between stable domains, and are not due to the specificity of the protease. For example, Tryp 6 and Prok 6 are similar COOH-terminal fragments of 96 and 114 amino acids, respectively, that were generated under specific nucleotide conditions. The accessibility of the NH_2-terminal region of these fragments to the protease varied depending on the presence of a nucleotide, suggesting that it may function like a hinge, separating adjacent domains that vary in their relative orientation. Another region targeted by both proteases and likely to function as a hinge is located between residues 155 and 160, defined by the NH_2 termini of Tryp 2 and Prok 2, and the COOH termini of Tryp 4, Tryp 5, and Prok 5.

Although the experiments with trypsin and proteinase K produced generally similar fragments and revealed some common domain structures, the conformational changes detected by trypsin are induced upon binding of any nucleotide, whereas those detected by proteinase K correspond to changes linked to ATP hydrolysis. Both PAN and the eukaryotic 19 S complex appear to undergo a cycle of changes in their functional properties depending on ATP binding and hydrolysis (6). The initial step in the function of these ATPases is the assumption of a polymeric ring structure. For homologous AAA family members (such as ClpA or HslU) nucleotide binding is an absolute prerequisite for ring formation (36). PAN, however, forms rings in the absence of any nucleotide and the nucleotide-dependent changes detected by trypsin probably correspond to further rearrangement of monomers into a functional conformation. A putative next step would be substrate binding. In studies with the peptide SsrA, specific, high affinity cross-linking to PAN occurred only when PAN was preincubated with ATPγS.[7] These findings together suggest that PAN assumes a unique conformation suitable for substrate binding when a non-hydrolyzable ATP analog is bound. This conformation is detected by proteinase K digestion of PAN bound to ATPγS, where the amino- and carboxyl-terminal domains are preserved, whereas the central region, including the Walker A and B motif, becomes protease-sensitive.

The next step in the ATPase cycle, substrate unfolding, is known to depend on ATP hydrolysis (6, 7). Thus, the conformational changes detected by proteinase K, which discriminates between the ATPγS and the ADP bound forms, correlate with these changes in function. We were unable to determine an affinity for ATPγS using proteinase K digestion as we did for nucleotide binding with trypsin. However, it is likely that this affinity corresponds to the 300–500 μM K_m determined previously for ATP dependence of protein breakdown. It is important to note that the ATP hydrolysis assay was conducted at 55 °C (300 μM K_m) or at 80 °C (500 μM K_m), whereas the protease sensitivity assays were run at 20 °C, and thus these values cannot be directly compared. However, the existence of high ($K_a \sim 20-40$ μM) and low affinity constants ($K_m \sim 300$ μM) for

[6] C. Reis, D. M. Smith, and A. L. Goldberg, unpublished observations.

[7] A. Navon, A. A. Horwitz, and A. L. Goldberg, manuscript in preparation.

FIGURE 6. **Proposed domain architecture of PAN and homology mapping to HslU.** *a*, schematic representation of domain architecture of Nsf-D2 (Chinese hamster), P97-D1 (*M. musculus*), and HslU (*E. coli*). The lengths of the shown protein fragments reflect their size. *Numbers below* HslU indicate the amino acid positions of its three different domains. NH_2-terminal (*blue*) and COOH-terminal (*green*) domains, show high homology and are structurally conserved among all members of the AAA^+ ATPases. In HslU the NH_2-terminal domain is split into two parts by an intermediate coiled-coil domain. *Beige* parts represent domains specific for each protein. Walker motifs are *boxed in red* and *blue*. *b*, ribbon-plot representation of the overall architecture of the three ATPase complexes. The orientation of the NH_2-terminal (*blue*) and COOH-terminal (*green*) domains in all three molecules is similar. COOH-terminal domains form tight contacts with NH_2-terminal domains of their adjacent subunits. Nucleotides always bind between the NH_2- and COOH-terminal domains and are depicted as ball-and-stick models (*red*). *c*, stereo representation of the structural superposition of the NH_2- and COOH-terminal domains of all three ATPases. The superpositioning was performed for C_α-atoms of the NH_2-terminal domains and the corresponding rotation matrix and translation vectors were applied to the whole subunit. All three subunits show a specific hinge region between NH_2- and COOH-terminal domains. Nucleotides (*red*) are oriented and positioned identically in all three structures. *d*, stereo representation of the HslU subunit topology. Each domain follows the specific color-coding as described in *a*. The NH_2 terminus is positioned in proximity of the intermediate coiled-coil domain, indicating a possible gene shuffling in PAN during evolution. *e*, proposed model for the overall architecture of PAN derived from the primary sequence comparison to HslU. The coiled-coil domain of PAN is transferred to its NH_2 terminus. The NH_2-terminal domain is not split, but located next to the COOH-terminal domain; the COOH-terminal domain itself is analogous to HslU. An additional domain (*black*) between the coiled-coil and the NH_2-terminal domain is present only in PAN. *Numbers below* the *box* indicate specific amino acid positions for the distinct domains. Tryptic cleavage sites are indicated by *blue* and proteinase K cleavage sites by *brown arrows*. Cleavage sites exposed or protected by nucleotides are highlighted against a *yellow background*.

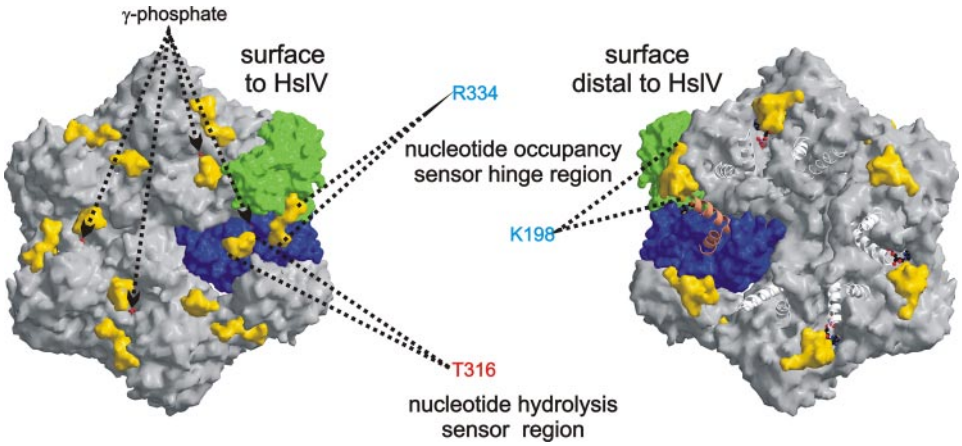

FIGURE 7. **Representation of the HslU-complex surface facing HslV.** Only four nucleotides were found in the crystal structure of HslU and two binding positions remained empty in accord with he present findings on PAN (Fig. 4). The NH_2- and COOH-terminal domains of one subunit are colored as before. The γ-phosphates of the nucleotides bound between the NH_2- and COOH-terminal domains are depicted in ball-and-stick models and are shown in *red*. *Yellow* surfaces represent the specific regions that have altered protection from proteases upon nucleotide binding in PAN. Cleavage sites are indicated. *Right panel*, surface representation of the HslU complex distal to HslV. The intermediate coiled-coil domains are only partially represented as ribbon plots to show the nucleotide.

ATP suggests that hydrolysis of ATP to ADP may introduce a negative effect on further ATP binding, especially if the affinity of ADP is higher than that of ATP. Thus the K_m of ATP may actually reflect the K_d of ADP, and because ATP is not hydrolyzed at 20 °C, this K_a is probably a more accurate estimate of ATP affinity.

Modeling the Structural Basis of These Conformational Transitions—To develop a model for PAN function that could be tested by mutagenesis, we examined the x-ray structures of three related AAA ATPase complexes, NSF-D2 (20, 37), p97-D1 (38), and HslU (21, 39, 40) (Fig. 6*B*). NSF-D2 (Chinese hamster), p97-D1 (*Mus musculus*), and HslU (*E. coli*) share high sequence homology in their amino- and carboxyl-terminal domains (Fig. 6*A*). Despite their relatively low overall sequence homology (~30%), structural comparisons of these proteins indicate a universal architecture of the AAA^+ fold (Fig. 6*C*). We chose to focus on HslU, which is the regulatory component of the HslUV complex (the *E. coli* homolog of the eukaryotic proteasome). Although related, HslU and PAN have clear differences in their primary sequences and domain organizations. In PAN, the coiled-coil domain resides in the extreme amino terminus of the molecule (residues 40–100), whereas in HslU this domain is in amino acids 96–251, inserted between Walker A and B motifs (Fig. 6*A*). The structure of HslU reveals that this insertion does not spatially disrupt the Walker AB motif because the coiled-coil domain is looped out, allowing arrangement of the Walker A and B motif (Fig. 6*D*). It seems likely that this alternate domain organization resulted from a gene-shuffling event that relocated the coiled-coil domain (21).

To examine this possibility, we compared the homology between PAN and HslU sequences before and after rearrangement of the HslU sequence to place the coiled-coil domain at the beginning of the NH_2 terminus. Upon rearrangement of the HslU sequence to match the domain organization of PAN, the homology between the sequences increased from ~25 to ~35%. Furthermore, our recent electron micrograph studies of PAN in complex with the 20 S reveal a basal ring plus an outer "pseudo ring" that seems to correspond to the coiled-coil domain (6), and resembles electron micrographs of HslUV (36). The putative domain structure of PAN was determined and is shown with sites of protease digestion (Fig. 6*E*). Using the improved alignment of PAN and HslU, we can localize the regions on the structure of HslU that probably correspond to sites of protease sensitivity in PAN (Fig. 7).

The two sites in PAN sensitive to nucleotide binding detected with trypsin were mapped to the structure of HslU. In the presence of nucleotide, trypsin cuts at Lys^{198} to produce Tryp 3. On the structure of HslU, this cut would occur in close proximity to the Walker A and B motifs and the bound nucleotide. Thus, cleavage at Lys^{198} most likely represents a local effect associated with nucleotide occupancy. In the HslU structure, four of the six subunits are bound to a nucleotide (21), as was found here for PAN. As noted above, overlap in the fragments generated upon trypsin digestion makes it likely that the PAN ring also contains both bound and unbound subunits. In addition to its proximity to the Walker A and B motifs, Lys^{198} is a particularly interesting location for a nucleotide-sensitive conformational change to occur. In a separate study, we have localized the substrate-binding site in PAN to the coiled-coil region, and the conformational changes detected here may reflect how substrate binding and ATP hydrolysis are linked.

The second nucleotide-sensitive fragment, Tryp 6, produced by a cut at Arg^{334}, was observed only in the absence of a nucleotide. On the sequence of PAN, it seems most likely that this cut occurs in a hinge region that connects a COOH-terminal domain to the NH_2-terminal domain. When modeled onto the structure of HslU, this cut would correspond to a short loop region between the COOH-terminal and NH_2-terminal domains. In HslU and the solved structures of related AAA members, the helical C-domain of one subunit embraces the nucleotide binding N-domain of the neighboring subunit in a counterclockwise orientation (Fig. 6*B*). Thus, the local conformational changes (*e.g.* Tryp 3) detected in this study presumably correspond to rearrangements in the Walker A and B motif of the individual monomer, whereas the global changes detected (*e.g.* Tryp 6) may correspond to alterations in the relative orientation of the monomers, *i.e.* structural rearrangements of the polymer ring.

In proteinase K digests, the COOH-terminal fragment generated in the ATPγS-bound state (Prok 6, Thr^{316}) is similar in size to Tryp 6, but is sensitive to ATP hydrolysis instead of just nucleotide binding. In this case, the cut occurs at the base of a loop that lies between the NH_2- and COOH-terminal domains (Fig. 7). This loop, although distant in primary amino acid sequence from the Walker A and B motif, is near the γ-phosphate in the HslU structure. Due to the distances in the primary

sequence, we had initially classified this site as an example of a long range conformational change induced by ATP hydrolysis, but the spatial proximity evident in the structure of HslU that suggests this could be a local effect resulting from loss of the γ-phosphate of ATP during ATP hydrolysis.

In summary, these studies show that the proteasome-regulatory ATPase PAN undergoes distinct conformational changes upon nucleotide binding and ATP hydrolysis. Although the conclusions drawn from modeling sites of protease sensitivity in PAN onto HslU are suggestive only, this analysis can inform future studies. We are currently using the structural information gained here to understand further the PAN reaction cycle and in the design of PAN deletion variants that are defective in substrate binding, unfolding, and translocation, and thus to gain a further understanding of the function of this proteasome-regulatory ATPase.

Acknowledgments—We thank Eran Or for help in designing the protease protection assays. We thank Jeffrey Parvin for support of one of us (A. A. H.).

REFERENCES

1. Ciechanover, A. (2005) *Nat. Rev. Mol. Cell. Biol.* **6,** 79–87
2. Benaroudj, N., Smith, D., and Goldberg, A. L. (2006) *The Ubiquitin Proteasome System*, WILEY-VCH Verlag GmbH & Co. KGaA, Weinheim, Germany
3. Coux, O., Tanaka, K., and Goldberg, A. L. (1996) *Annu. Rev. Biochem.* **65,** 801–847
4. Voges, D., Zwickl, P., and Baumeister, W. (1999) *Annu. Rev. Biochem.* **68,** 1015–1068
5. Kohler, A., Cascio, P., Leggett, D. S., Woo, K. M., Goldberg, A. L., and Finley, D. (2001) *Mol. Cell* **7,** 1143–1152
6. Smith, D. M., Kafri, G., Cheng, Y., Ng, D., Walz, T., and Goldberg, A. L. (2005) *Mol. Cell* **20,** 687–698
7. Benaroudj, N., Zwickl, P., Seemuller, E., Baumeister, W., and Goldberg, A. L. (2003) *Mol. Cell* **11,** 69–78
8. Lam, Y. A., Lawson, T. G., Velayutham, M., Zweier, J. L., and Pickart, C. M. (2002) *Nature* **416,** 763–767
9. Navon, A., and Goldberg, A. L. (2001) *Mol. Cell* **8,** 1339–1349
10. Groll, M., Bajorek, M., Kohler, A., Moroder, L., Rubin, D. M., Huber, R., Glickman, M. H., and Finley, D. (2000) *Nat. Struct. Biol.* **7,** 1062–1067
11. Zwickl, P., Ng, D., Woo, K. M., Klenk, H. P., and Goldberg, A. L. (1999) *J. Biol. Chem.* **274,** 26008–26014
12. Lowe, J., Stock, D., Jap, B., Zwickl, P., Baumeister, W., and Huber, R. (1995) *Science* **268,** 533–539
13. Akopian, T. N., Kisselev, A. F., and Goldberg, A. L. (1997) *J. Biol. Chem.* **272,** 1791–1798
14. Kisselev, A. F., Akopian, T. N., and Goldberg, A. L. (1998) *J. Biol. Chem.* **273,** 1982–1989
15. Strickland, E., Hakala, K., Thomas, P. J., and DeMartino, G. N. (2000) *J. Biol. Chem.* **275,** 5565–5572
16. Braun, B. C., Glickman, M., Kraft, R., Dahlmann, B., Kloetzel, P. M., Finley, D., and Schmidt, M. (1999) *Nat. Cell Biol.* **1,** 221–226
17. Benaroudj, N., and Goldberg, A. L. (2000) *Nat. Cell Biol.* **2,** 833–839
18. Baumeister, W., Walz, J., Zuhl, F., and Seemuller, E. (1998) *Cell* **92,** 367–380
19. Larsen, C. N., and Finley, D. (1997) *Cell* **91,** 431–434
20. Lenzen, C. U., Steinmann, D., Whiteheart, S. W., and Weis, W. I. (1998) *Cell* **94,** 525–536
21. Bochtler, M., Hartmann, C., Song, H. K., Bourenkov, G. P., Bartunik, H. D., and Huber, R. (2000) *Nature* **403,** 800–805
22. Guenther, B., Onrust, R., Sali, A., O'Donnell, M., and Kuriyan, J. (1997) *Cell* **91,** 335–345
23. Confalonieri, F., and Duguet, M. (1995) *Bioessays* **17,** 639–650
24. Patel, S., and Latterich, M. (1998) *Trends Cell Biol.* **8,** 65–71
25. Davy, A., Bello, P., Thierry-Mieg, N., Vaglio, P., Hitti, J., Doucette-Stamm, L., Thierry-Mieg, D., Reboul, J., Boulton, S., Walhout, A. J., Coux, O., and Vidal, M. (2001) *EMBO Rep.* **2,** 821–828
26. Sharon, M., Taverner, T., Ambroggio, X. I., Deshaies, R. J., and Robinson, C. V. (2006) *PLoS Biol.* **4,** 1314–1323
27. Fu, H., Reis, N., Lee, Y., Glickman, M. H., and Vierstra, R. D. (2001) *EMBO J.* **20,** 7096–7107
28. Hartmann-Petersen, R., Tanaka, K., and Hendil, K. B. (2001) *Arch. Biochem. Biophys.* **386,** 89–94
29. Glickman, M. H., Rubin, D. M., Coux, O., Wefes, I., Pfeifer, G., Cjeka, Z., Baumeister, W., Fried, V. A., and Finley, D. (1998) *Cell* **94,** 615–623
30. Menon, A. S., and Goldberg, A. L. (1987) *J. Biol. Chem.* **262,** 14921–14928
31. Wilson, H. L., Ou, M. S., Aldrich, H. C., and Maupin-Furlow, J. (2000) *J. Bacteriol.* **182,** 1680–1692
32. Hartman, J. J., and Vale, R. D. (1999) *Science* **286,** 782–785
33. Babst, M., Wendland, B., Estepa, E. J., and Emr, S. D. (1998) *EMBO J.* **17,** 2982–2993
34. Whiteheart, S. W., Rossnagel, K., Buhrow, S. A., Brunner, M., Jaenicke, R., and Rothman, J. E. (1994) *J. Cell Biol.* **126,** 945–954
35. Hersch, G. L., Burton, R. E., Bolon, D. N., Baker, T. A., and Sauer, R. T. (2005) *Cell* **121,** 1017–1027
36. Rohrwild, M., Pfeifer, G., Santarius, U., Muller, S. A., Huang, H. C., Engel, A., Baumeister, W., and Goldberg, A. L. (1997) *Nat. Struct. Biol.* **4,** 133–139
37. Yu, R. C., Hanson, P. I., Jahn, R., and Brunger, A. T. (1998) *Nat. Struct. Biol.* **5,** 803–811
38. Zhang, X., Shaw, A., Bates, P. A., Newman, R. H., Gowen, B., Orlova, E., Gorman, M. A., Kondo, H., Dokurno, P., Lally, J., Leonard, G., Meyer, H., van Heel, M., and Freemont, P. S. (2000) *Mol. Cell* **6,** 1473–1484
39. Wang, J., Song, J. J., Seong, I. S., Franklin, M. C., Kamtekar, S., Eom, S. H., and Chung, C. H. (2001) *Structure* **9,** 1107–1116
40. Sousa, M. C., Trame, C. B., Tsuruta, H., Wilbanks, S. M., Reddy, V. S., and McKay, D. B. (2000) *Cell* **103,** 633–643

ATP-induced Structural Transitions in PAN, the Proteasome-regulatory ATPase Complex in Archaea

Andrew A. Horwitz, Ami Navon, Michael Groll, David M. Smith, Christian Reis and Alfred L. Goldberg

J. Biol. Chem. 2007, 282:22921-22929.
doi: 10.1074/jbc.M702846200 originally published online June 6, 2007
